ELSEVIER

Ceramics International 25 (1999) 77–84

CERAMICS
INTERNATIONAL

Low thermal expansion refractory composites based on $CaAl_4O_7$

S. Jonas[a,*], F. Nadachowski[a], D. Szwagierczak[b]

[a] *Academy of Mining and Metallurgy, Al Mickiewicza 30, Cracow, Poland*
[b] *Research and Development Centre for Hybrid Microelectronics and Resistors, Cracow, Poland*

Received 24 November 1997; accepted 7 January 1998

Abstract

Following the previously reported elaboration of low thermal expansion refractory composites based on $CaAl_4O_7$, further compositions of this type are presented. They are principally based on combinations of $CaAl_4O_7$ with $MgAl_2O_4$; also, complementary data relating to those with $CaZrO_3$ are given. Specially adjusted bimodal particle size distributions were applied: granular fractions (0.09–0.5 mm) of the spinel and the zirconate embedded in fine (under 0.06) calcium dialuminate matrices. It could be shown that composites with up to more than 50% volume content of $MgAl_2O_4$ and $CaZrO_3$ grains will retain the merit of low expansion coefficients imposed by the matrix in spite of the much higher values of this property characteristic of both the granular constituents. A peculiar phenomenon of expansion even lower than that of $CaAl_4O_7$ itself was observed, too. The rather complex relations between the thermal expansion and composition/microstructure features are discussed and some relevant definitions are proposed. The added two minerals contributing to the favourable behaviour of the composites as a whole are fully compatible at high temperatures with the dialuminate. Interpretation of SEM and EPMA data for two representative compositions (with ca. one half of spinel and zirconate volume content) is presented; also, some technological implications are indicated. © 1998 Published by Elsevier Science Limited and Techna S.r.l. All rights reserved.

1. Introduction

Following our preliminary testing of calcium dialuminate (= CA_2) as a refractory of low thermal expansion [1], further investigations of composites showing similar merits were undertaken in the present work. The basic consideration underlying these studies has been that a CA_2 matrix can to some extent impose its low value of the thermal expansion coefficient α on the composite as a whole. $CaAl_4O_7$ fully synthesized from Al_2O_3 and $CaCO_3$ by repeated firing operations by Criado and de Aza [2] has shown an astonishingly low thermal expansion coefficient—especially at low temperatures. This finding might be compared with that of Sulikowski and Sawków [3] who used a single firing operation at 1500°C to obtain CA_2 from technical raw materials, obviously leaving in their product some amounts of phases other than the dialuminate. Still, the expansion data of this 'incomplete' CA_2 were low enough to be interesting from the technological point of view. So were the α values of the dialuminate with some $CaAl_2O_4$ (= CA) contamination prepared by us [1]. Fine-grained mixtures of this dialuminate with the similarly synthesized $CaZrO_3$ (compatible with CA_2 at high temperatures [4,5]) turned out to be a promising refractory composite. In the present work, attention was also focused on another high-melting component—the spinel $MgAl_2O_4$ (= MA), known to be widely used in refractory monolithics as well as fired products. As can be seen from the phase diagram in Fig. 1, MA is also fully compatible with CA_2. The combinations of these two phases are highly refractory, developing a liquid phase only above 1700°C; SiO2 contamination forming gehlenite $Ca_2Al_2SiO_7$ has to be avoided.

The advantage of the low thermal expansion of calcium dialuminate anticipating an excellent thermal shock resistance can be utilized in refractory composites to a remarkable extent. The precondition of this is that grain size distribution of the mixture be adjusted so that the continuous CA_2 matrix will surround larger, dispersed and isolated grains of the other constituent (the one showing higher α values, but also a higher melting point). This type of particle configuration will further be referred to as 'bimodal microstructure'—according to the shape of the grain size distribution curve which is characterized by two modal values.

---

[*] Corresponding author.

0272-8842/98/$—see front matter ©1998 Published by Elsevier Science Limited and Techna S.r.l. All rights reserved
PII: S0272-8842(98)00004-2

2. Experimental procedures, materials and compositions

The procedure for synthesizing $CaAl_4O_7$ and $CaZrO_3$ from reagents: $CaCO_3$, Al_2O_3 and ZrO_2 was described in detail previously [1]. In short, they were prepared by double or triple firing followed by regrinding, the last (maximal) firing temperature having been 1450°C. X-ray phase analysis had indicated some CA contamination in CA_2; this is shown in Fig. 2.

The spinel used in the present experiments was a commercial fused material containing $>97\%$ $MgO+Al_2O_3$, the impurities being mainly CaO, SiO_2 and Fe_2O_3. True densities of the synthesized minerals were determined on pulverized samples using the Micrometrics Accupyc 1330 device. General characteristics of the three components forming the mixtures of this work are given in Table 1, some data having been taken from our previous publication [1].

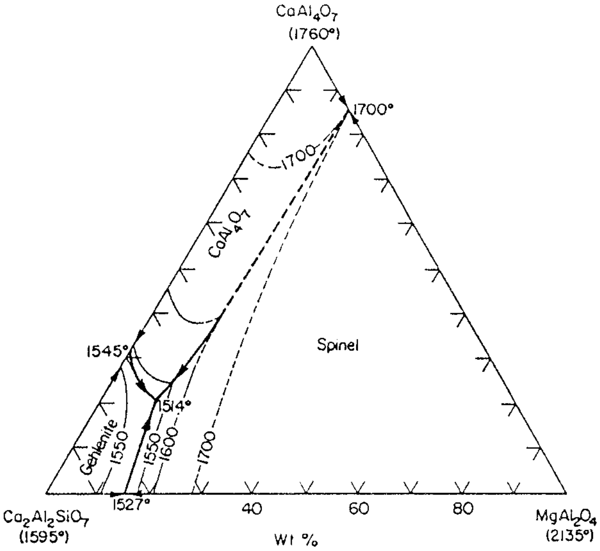

Fig. 1. System $CaAl_4O_7$–$MgAl_2O_4$ (spinel)–$Ca_2Al_2SiO_7$ (gehlenite), ternary [6].

The experimental compositions were formulated using two fractions of the starting components: (1) the fine fraction under 0.06 mm and (2) the granular fraction 0.09–0.5 mm, screened out of the crushed briquettes of sintered CA_2 and CZ and fused MA grains. Fraction (1) was destined to form the continuous matrix, and fraction (2)—the isolated larger grains in the microstructure of the experimental bodies. The type of particle size distribution mainly used in the present work (according to the outlined concept of minimizing the α coefficients) is further referred to as the 'bimodal proper' (BP) configuration. The feature of being 'proper' means here causing favourable deviations from the composite mixture rule (net expansions lower than expected). In the BP type microstructures the matrix was always CA_2, while the constituents of higher α values (MA and CZ) were taken as granular fractions.

Table 1
Characteristics of the components of the experimental mixtures

Designation	Chemical formula and melting point (°C)	True density (gcm^{-3})	Remarks
CA_2	$CaAl_4O_7$ 1760	3.00	Laboratory synthesis according to [1]
CZ	$CaZrO_3$ 2345	4.90	As above
MA	$MgAl_2O_4$ 2135	3.75	Commercial fused material ($>97\%MgO+Al_2O_3$ [a])

[a] 34.35–38.96% MgO; 0.42–0.96% SiO_2; 59.40–63.25% Al_2O_3; 0.29–0.59% Fe_2O_3; 0.88–1.21% CaO.

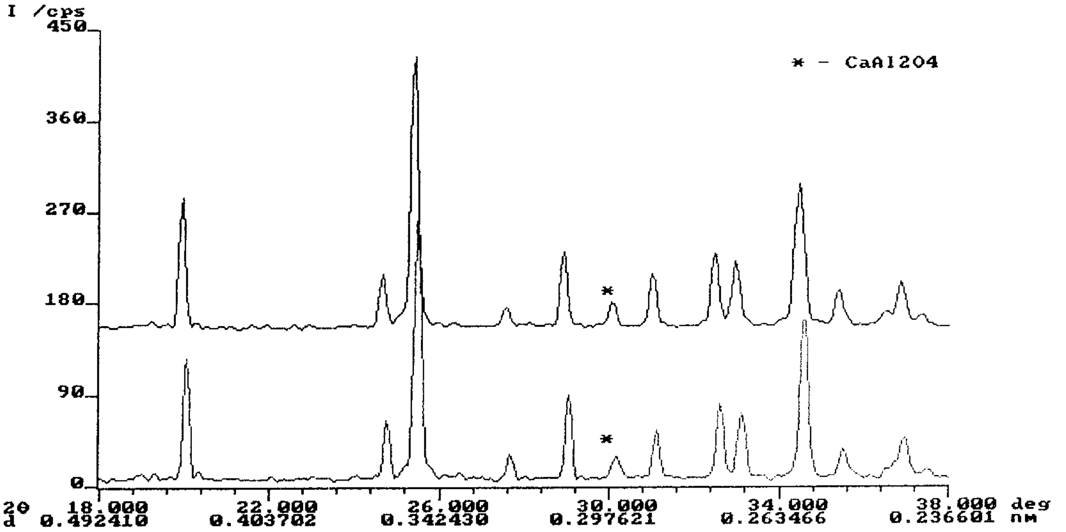

Fig. 2. X-ray diffraction pattern of two samples of synthesized $CaAl_4O_7$, believed to contain some amount of $CaAl_2O_4$ (peak marked by asterisk).

In order to expose, by contrasting comparison, the effect of the BP configurations, a 'reversed' bimodal microstructure type (= BR) was also tried-out for a few selected compositions. The BR specimens were in that case built-up of fine MA or CZ matrices in which the granular fraction of sintered CA_2 was embedded. To complete the comparison, some fine-grained microstructures previously prepared [1] were also included in this experimental series. The compositions are listed in Table 2, with their volume proportions and microstructure types indicated.

The prepared mixtures of Table 2 were pressed into rods of ca. 7 mm diameter and ca. 20 mm height and sintered at 1500°C (held during 0.5 h). Their mean thermal expansion coefficients α_m were measured in the temperature range 20-900°C (registered each 100°C) using a high temperature dilatometer (Linseis Messgeräte), with silica glass elements. Apparent porosities and bulk densities of selected fired specimens were determined in kerosene according to the Polish standard method PN-64H/-04185. Also, microscopic examinations using SEM and EPMA images were made.

3. Results

Mean thermal expansion coefficients for the compositions 1–15 are listed in Table 3 and depicted in Fig. 3. For two important CA_2/MA compositions (Nos 5 and 6 from Table 3), the measurements were repeated independently, showing good reproducibility. Plots illustrating the changes of α values as a function of MA volume content in CA_2/MA composites for three temperatures chosen (200, 500 and 900°C) are shown in Fig. 4. In Fig. 5 fragments of the composites No. 4 and No. 12 exemplifying their microstructures (grain/matrix boundary) are presented. Porosity data of the composites are given in Table 4. Further scanning electron micrographs as well as electron probe microanalyses extending the composition study of the two selected specimens are presented in Figs. 6–9.

Table 2
Experimental compositions

No.	Percent weight proportions	Percent volume proportions		Microstructure (fraction configuration) type
		Fine fraction (< 0.06 mm)	Granular fraction (0.09–0.5 mm)	
1	100 CA_2	100 CA_2	–	FG
2	100 MA	100 MA	–	FG
3	100 CZ	100 CZ	–	FG
4	50 CA_2/50 MA	55.5 CA_2	45.5 MA	BP
5	40 CA_2/60 MA	45.5 CA_2	54.5 MA	BP
6	35 CA_2/65 MA	40 CA_2	60MA	BP
7	30 CA_2/70 MA	35 CA_2	65 MA	BP
8	20 CA_2/80 MA	24 CA_2	76 MA	BP
9	50 CA_2/50 MA	45.5 MA	55.5 CA_2	BR
10	40 CA_2/60 MA	54.5 MA	45.5 CA_2	BR
11	50 CA_2/50 CZ	62 CA_2	38 CZ	BP
12	40 CA_2/60 CZ	52 CA_2	48 CZ	BP
13	50 CA_2/50 CZ	38 CZ	62 CA_2	BR
14	40 CA_2/60 CZ	48 CZ	52 CA_2	BR
15	50 CA_2/50 CZ	62 CA_2/38 CZ	–	FG

4. Discussion

A general assessment of the expansion data given in Table 3 and Figs. 3 and 4 confirms the declared feasibility of developing low thermal expansion composites containing $MgAl_2O_4$ and $CaZrO_3$ granular fractions

Table 3
Thermal expansion data for compositions of Table 2

Composition, No.	Mean linear expansion coefficient [$\alpha_m.10^6$, °C^{-1}] up to temperature (°C)								
	100	200	300	400	500	600	700	800	900
1	1.2	2.1	2.5	2.9	3.2	3.4	3.7	3.9	4.1
2	4.4	6.1	6.8	7.5	7.8	8.0	8.2	8.3	8.5
3	6.5	7.7	8.2	8.3	8.4	8.5	8.5	8.5	8.5
4	0.9	1.8	2.2	2.7	3.1	3.4	3.7	3.9	4.2
5[a]	1.0	1.7	2.2	2.8	3.1	3.5	3.7	3.9	4.2
6[b]	2.8	3.7	3.6	4.3	4.3	4.6	4.7	5.0	5.2
7	3.0	4.1	4.4	4.9	5.2	5.4	5.6	5.8	5.9
8	4.0	5.5	6.0	6.7	6.9	7.0	7.1	7.2	7.3
9	3.0	4.0	4.2	4.3	4.6	4.8	5.0	5.1	5.3
10	3.8	4.7	4.7	4.8	5.0	5.2	5.3	5.5	5.7
11	0.7	1.2	1.7	2.2	2.6	3.0	3.3	3.4	3.6
12	1.2	1.6	1.9	2.5	2.8	3.1	3.3	3.5	3.8
13	2.9	4.3	4.6	4.8	4.5	4.5	4.5	4.6	4.7
14	3.8	4.8	5.1	5.2	5.3	5.4	5.5	5.6	5.6
15	3.4	4.0	4.4	4.6	4.9	5.0	5.2	5.3	5.4

[a] Mean values, three independent measurements.

[b] Mean values, two independent measurements.

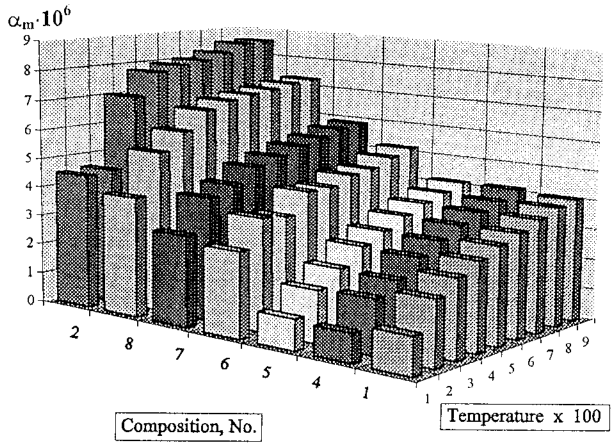

Fig. 3. Thermal expansion coefficients ($\alpha_m.10^6$) of compositions of Table 2 (weight proportions).

embedded in a $CaAl_4O_7$ matrix. The obtained α values are particularly favourable at low temperatures—typically around 2.10^{-6} °C^{-1} at 200°C, rising to ca. 3.10^{-6} °C^{-1} at 500°C and 4.10^{-6} °C^{-1} at 900°C. The finding most important technologically is that on introducing even more than one half volume content of MA or CZ grains into the composite body, it is still the fine-grained CA_2 component which extends its low expansion feature on the fired specimens as a whole. This is in total disagreement with the mixture rule (corresponding to straight dashed lines connecting the α values for CA_2, MA and CZ in Fig. 4); this rule would require average α_m values—e.g. 4–5.10^{-6} °C^{-1} at 200°C instead ca. 2.10^{-6} °C^{-1}. The observed advantage will be called here the "particle size bimodality effect" (=PSBE); it relates to combinations of up to 50–60% of fractions 0.09–0.5 mm (or possibly coarser ones) of the minerals of medium or high inherent thermal expansion, with pulverized (under 0.06 mm or finer) CA_2 matrices. Characteristic of these combinations is that on further enhancing the contents of the granular fractions—beyond the range of the BP compositions—there occurs an abrupt increase of the α values of the composites. This constitutes, as it were, a return to accordance with the mixing rule, which is obviously due to the increasing discontinuity of the matrix—as its volume content approaches and then falls beneath the level of 35–25%. The curves in Fig. 4 exemplify the described type of the dependence of thermal expansion on composition. Generally, the reported data indicate that low expansion composites can be elaborated using technical materials, in particular calcium dialuminate synthesized by simplified procedures and not yet fully equilibrated (i.e. containing residual amounts of unreacted CA—as indicated in Table 1). The two kinds of granular components used in this experimental series are fairly different not only chemically, but

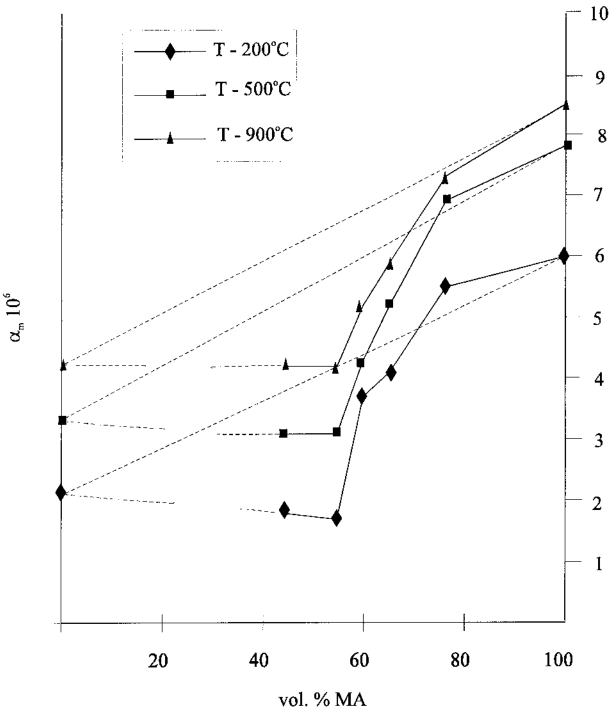

Fig. 4. Curves showing the dependence of thermal expansion coefficients ($\alpha_m.10^6$) on volume content of the spinel granular fraction in CA_2/MA composites for temperatures: 200, 500 and 900°C. Dashed straight lines represent the levels of α_m values which would correspond to the mixture rule.

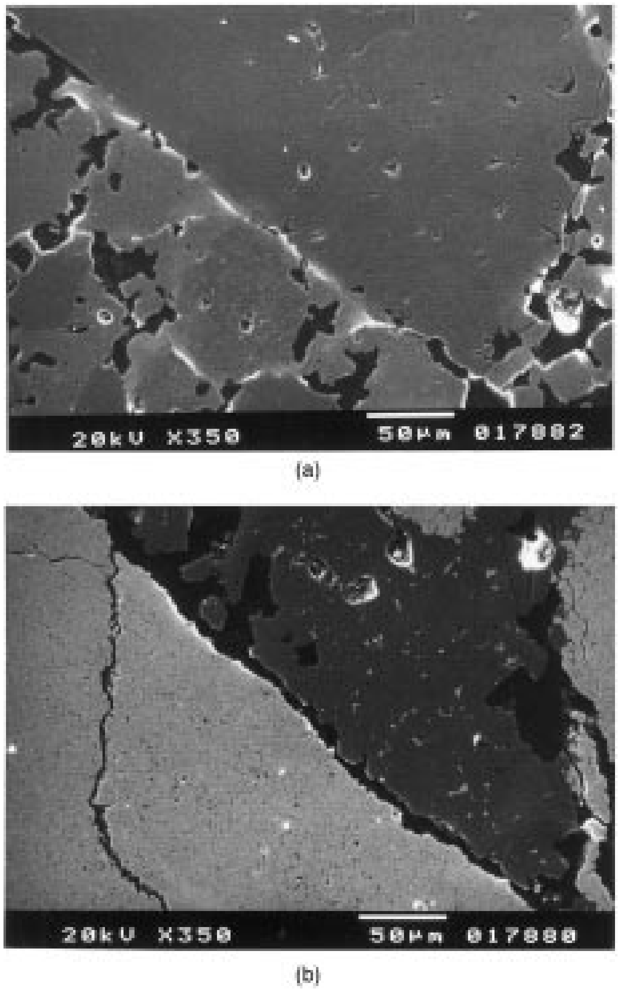

Fig. 5. SEM pictures of two selected specimens of near-equal proportions of the CA_2 matrix and the granular fractions of MA and CZ: (a) composition No. 4, the MA grain in the upper-right part, (b) composition No. 12, the CZ grain in the lower-left part.

Table 4
Porosity data of two selected compositions

Composition No.	Apparent porosity (vol.%)	Bulk density (g.cm^{-3})	Estimated closed porosity (vol.%)
4	18.2	2.33	13
12	12.9	2.98	13

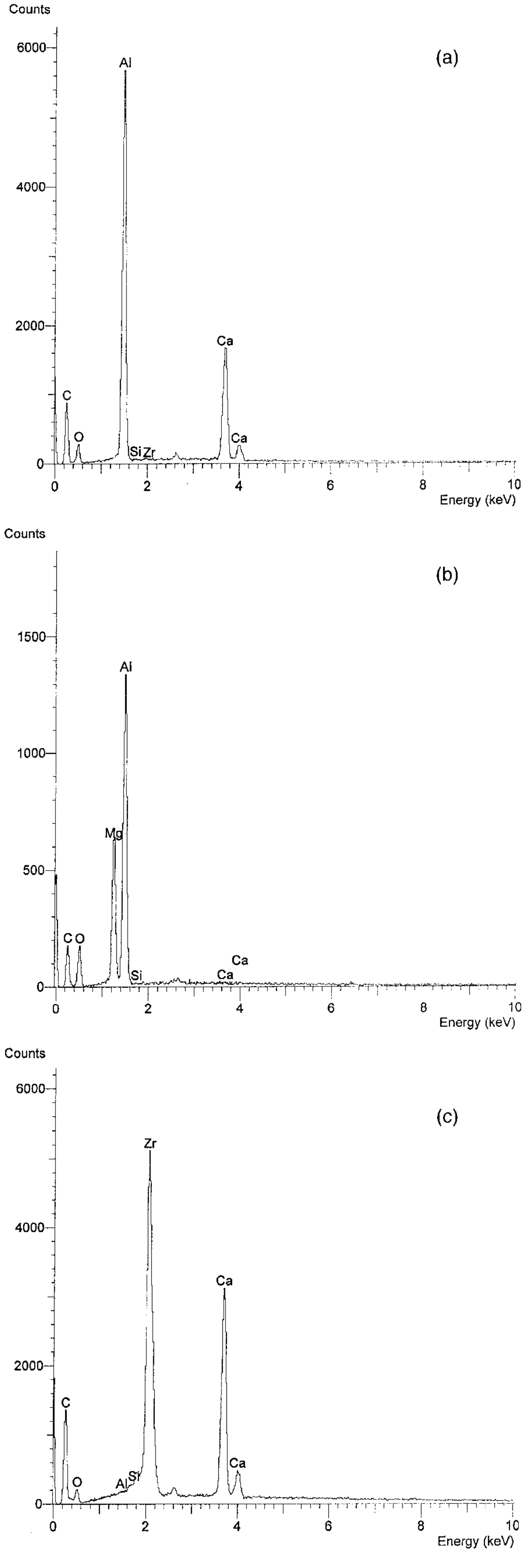

Fig. 6. EPMA spot analyses of the particles of mineral constituents of the experimental compositions: (a) CA_2, (b) MA, (c) CZ.

also in their general microstructures. The MA consists of angular fused grains often containing scattered closed pores, while the CA_2 is a set of sintered aggregates of tiny (micron-size) oval crystallites [cf. Figs. 8(a) and 9(a)]. It should be noted that the microstructure of the CA_2 matrices considered separately in both the composite types differs as well—especially with regard to the amount and morphology of the intergranular pores (also reflected, to some extent, by the data of Table 4). These differences apparently do not affect the very occurrence of the 'bimodality effect', but may complicate its nature. So may the observed presence of a small amount of MA grains finer than 0.06 mm in the

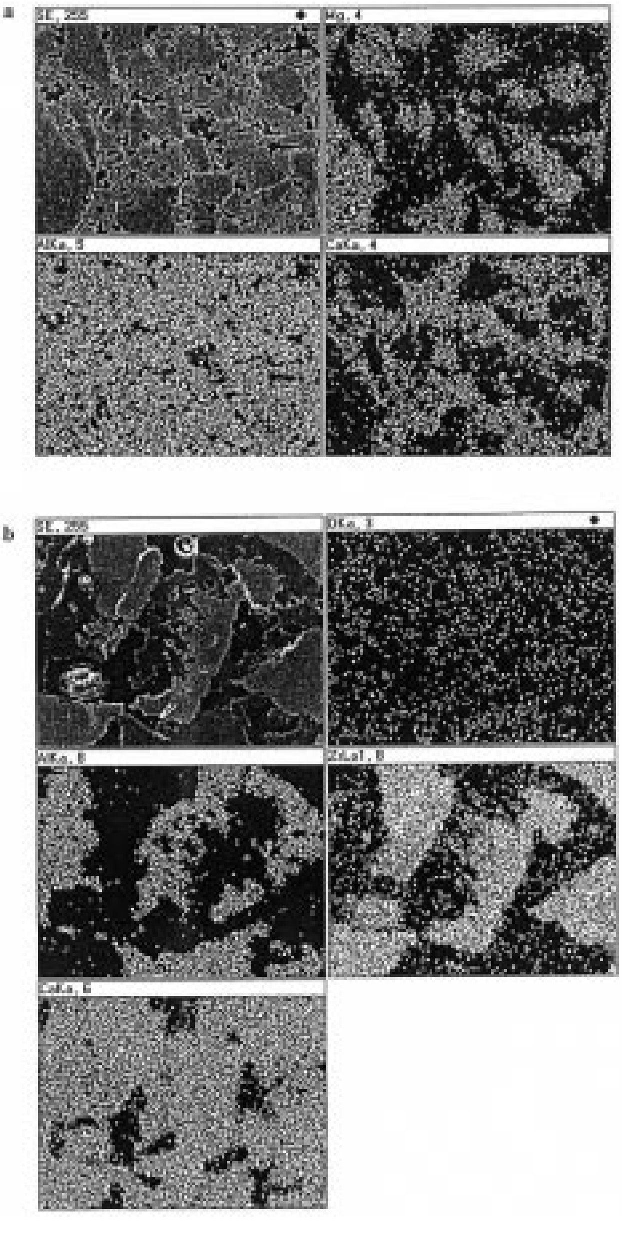

Fig. 7. SEM images and elemental distribution maps of specimens: (a) No. 4, (b) No. 12.

CA_2/MA specimens or the dissipation of some tiny CZ crystals into the matrix of CA_2/CZ ones (see further Fig. 7). Quantitatively, the overall PSBE can be established as the difference (expressed in $\alpha.10^6$ values) between the relevant point on the straight line connecting the α values of single constituents (the line representing the mixture rule), and the values measured experimentally, for the given composition and temperature. Analyzing the nature of the observed effect, one will distinguish two subeffects whose sum makes up the resulting PSBE magnitude. The first of these subeffects (the prepondering one) can be described as the absence or delay of the expected increments of the α values (over those established for CA_2). These increments should theoretically take place according to the mixture rule as the granular fraction of MA or CZ is added to the fine-grained aluminate. The subeffect thus defined will be equal to the difference between the considered point on the mentioned straight line and the α values of CA_2. It resembles the hysteresis effect occurring with some systems of physical properties and will be called here the 'expansion increment hysteresis' (=EIH). The other subeffect of the total PSBE magnitude results from the peculiar phenomenon of a distinct decrease of the initial (already low!) α value of CA_2; it follows the addition of the granular fraction of a mineral of much higher thermal expansion. The nature of this effect may be formulated as damping the inherent property of the CA_2 matrix to expand on heating or, in short, MED ('matrix expansion damping'). The bimodality effect data are fitted into a diagram in Fig. 10 constructed to show the range and changing magnitude of PSBE for both MA and CZ composite series (in comparison with the α values of the 'reversed' and 'fine-grained' specimens). It is significant that pronounced hysteresis effects (EIH) range as far as near 60 vol% of MA in the composite bodies. Thus, even with the CA_2 matrix constituting less than one half of the composite volume, it is still capable of imposing its low expansion merit on the material as a whole. This is not so in the 'reversed' compositions where there is no sign of the logically

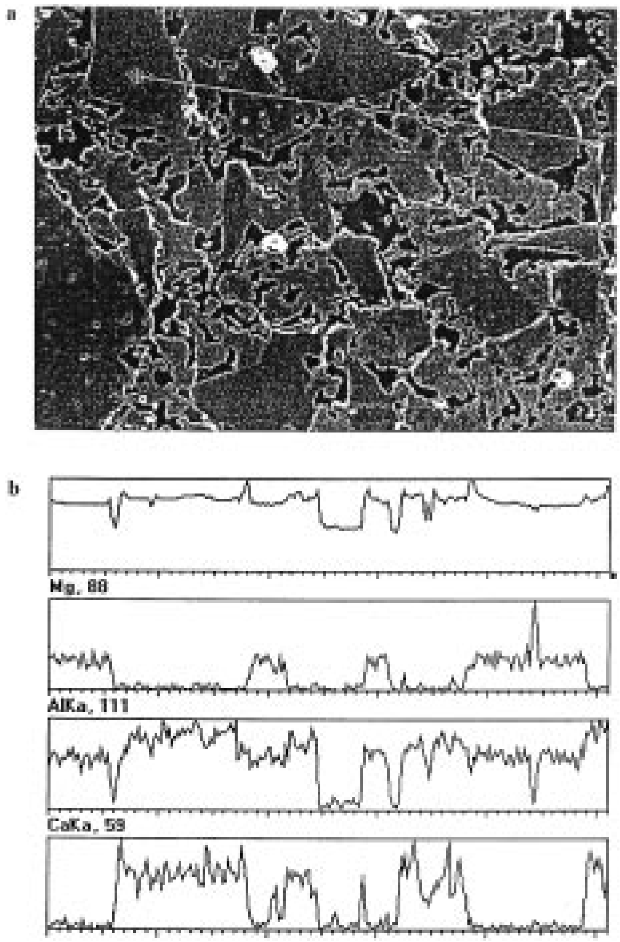

Fig. 8. SEM image (a) and line analyses (b) of specimen No. 4.

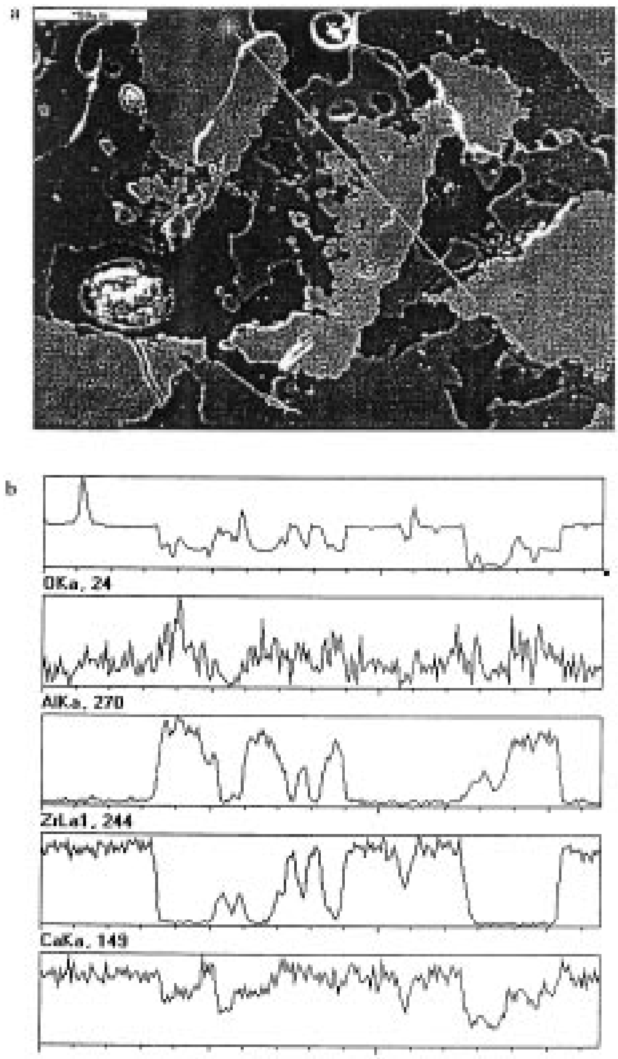

Fig. 9. SEM image (a) and line analyses (b) of specimen No. 12.

anticipated ‘symmetry’ in the phenomenon of matrices ‘governing’ the α values; these are scattered rather below the zero level instead of being much higher.

As to the astonishing MED phenomenon, it turned out to be most impressive in the CZ/CA_2 series, at fairly low CZ contents, at low temperatures; it can reach even one half of the inherent α value for CA_2. MED seems to deserve more extended studies. A factor in its mechanism may possibly be the formation of microfissures both at the grain/matrix boundaries, and across elongated CZ grains [cf. Figs. 5(b) and 9(a)].

Chemical compositions of the three constituent minerals contained in the specimens: CA_2, MA and CZ are clearly defined and correspond to their formulas. This is evident from the spot analyses given in Figs. 6(a–c), and identifying the grains noticed in the examined microstructures. The basis for the identification are the peaks ascribed to elements Al, Ca, Mg and Zr, the last two being useful in distinguishing between the granular constituents (the spinel and the zirconate) and the Ca–dialuminate matrix. The Si contamination is negligible. In Figs. 7–9 no distinct domains of an interaction or mutual diffusion of different species between the adjacent fragments of the presented microstructures could be observed. This renders improbable any transitional formation of ternary non-equilibrium phases, such as the low melting $3CaO.MgO.2Al_2O_3$, known from the phase diagram by Majumdar [7], or the compound $7CaO.3Al_2O_3.ZrO_2$ reported by Melnik et al. [5]. There is no indication, too, of a possible penetration of Ca into the $MgAl_2O_4$ lattice, Mg into $CaAl_4O_7$, or Al into $CaZrO_3$. Thus, in elaborating further compositions and technological variants along this line, the CA_2 matrices and the granular constituents ought to be regarded as separate subsystems of rather contrasting physical behaviour, contributing in a complex way to the thermal expansion of composite material. However, the expansion will not be affected by any tangible mutual influence of chemical nature, up to very high service temperatures. The data accumulated so far should help to better outline the potential refractory applications of the CA_2-based, non-silicate composites. One of these would be the submerged nozzles in the continuous casting of steel, already suggested earlier [1]. More technological variants of refractory functional shapes can presumably be developed taking advantage of the astonishingly low thermal expansion of these new materials at temperatures up to the red-heat level. The commercially produced spinel as their potential constituent could extend the chances of application to linings of such large scale installations, as steel ladles and cement kilns.

For a general assessment, percent linear expansion curves of composites containing 50–60% spinel are

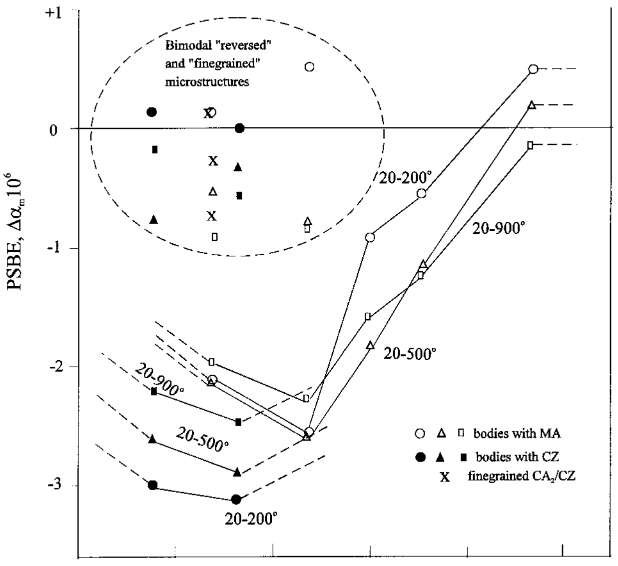

Fig. 10. Bimodality effect (PSBE) values (in negative $\alpha_m.10^6$ units) related to the corresponding average α_m values resulting from the mixture rule (interpreted as zero level on the diagram). The dependence of the negative magnitude of PSBE on volume proportions of the granular constituents is shown for three selected temperatures. Also, the area of α_m values of the ‘reversed’ and ‘fine-grained’ microstructures, located near the 0 level, is indicated.

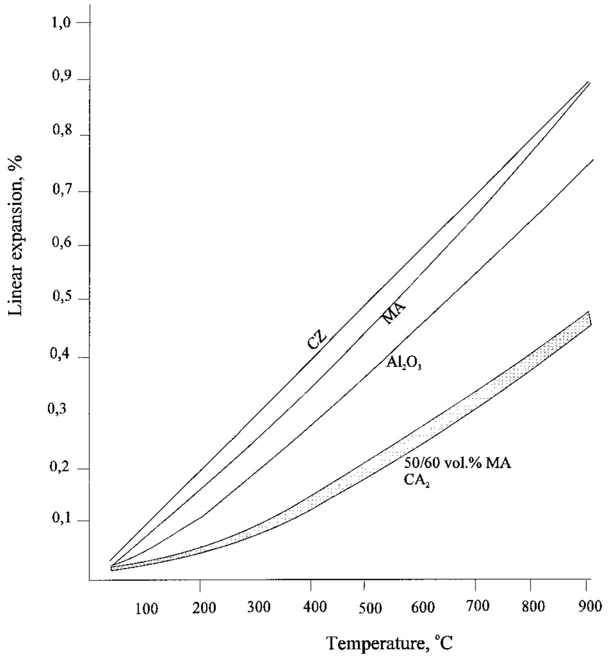

Fig. 11. α_m values as a function of temperature of some compositions of Table 3 recalculated to show percent linear expansion in comparison with those of $CaZrO_3$, $MgAl_2O_4$ and Al_2O_3. The dotted streak represents the range of data obtained for CA_2 and five independently repeated measurements for specimens containing 50% and 60% $MgAl_2O_4$.

shown in Fig. 11 along with those of single minerals (including corundum). The location of the narrow streak comprising several measurement series of these composites shows their merit of low α values, not exceeding those of CA_2.

5. Conclusions

As a further development of the new refractory materials based on $CaAl_4O_7$, compositions with granular fractions of $MgAl_2O_4$ and $CaZrO_3$ are proposed; both these high-melting minerals are fully compatible with the calcium dialuminate matrix. Remarkable effects of lowering the expansion which would be expected according to the mixing rule were attained, signalling the possibility of development of novel products of an excellent resistance to thermal shocks. In interpreting the behaviour on heating and the microstructures of the investigated composites, peculiar specific phenomena were described.

References

[1] S. Jonas, F. Nadachowski, D. Szwagierczak, A new non-silicate material of low thermal expansion. Ceramics International 24 (3) (1998) 211.

[2] E. Criado, S. De aza, Calcium hexaaluminates as refractory material. UNITECR Congress, Aachen, 1991, p.403.

[3] J. Sulikowski, J. Sawków, Dilatometry of refractory aluminous cements. Cement Wapno Gips XXIX/XLI (1974) (in Polish).

[4] P. Pena, S. De Aza, Compatibility relations of Al_2O_3 in the system ZrO_2–Al_2O_3–SiO_2–CaO, Journal American Ceramic Society 68 (1984) C3.

[5] M.T. Melnik, N.G. Ilyukha N.N. Shapovalova, Refractory cements, Vyssha shkola, Kiev, 1984, p. 77.

[6] M.R. Rao, Journal of the American Ceramic Society 51 (1) (1968) 51.

[7] A.J. Majumdar, Transactions of the British Ceramics Society 63 (7) (1964) 357.